

## Impacts of climate warming and permafrost thaw on the riverine transport of nitrogen and phosphorus to the Kara Sea

Karen E. Frey,<sup>1</sup> James W. McClelland,<sup>2</sup> Robert M. Holmes,<sup>3</sup> and Laurence C. Smith<sup>4</sup>

Received 13 November 2006; revised 8 April 2007; accepted 15 May 2007; published 26 October 2007.

[1] Measurements of nitrogen and phosphorus (N and P) concentrations from previously unstudied streams and rivers throughout west Siberia suggest that climate warming and/or associated permafrost thaw will likely amplify the transport of N and P to the Kara Sea and adjacent Arctic Ocean. We present concentrations of dissolved organic nitrogen (DON), ammonium (NH<sub>4</sub>-N), nitrate (NO<sub>3</sub>-N), total dissolved nitrogen (TDN), and total dissolved phosphorus (TDP) from 96 streams and rivers within the Ob'-Irtysh, Nadym, and Pur river drainage basins. The sampled sites span ~10<sup>6</sup> km<sup>2</sup>, a large climatic gradient (~55°N–68°N), and include 41 cold, permafrost-influenced and 55 warm, permafrost-free watersheds. Concentrations for all measured watersheds average 765 μg L<sup>-1</sup> (DON), 19.3 μg L<sup>-1</sup> (NH<sub>4</sub>-N), 36.7 μg L<sup>-1</sup> (NO<sub>3</sub>-N), 821 μg L<sup>-1</sup> (TDN), and 104 μg L<sup>-1</sup> (TDP). Our results show no statistically significant difference in dissolved inorganic N (NH<sub>4</sub>-N and NO<sub>3</sub>-N) between permafrost-influenced and permafrost-free watersheds. However, we do find significantly higher concentrations of DON, TDN, and TDP in permafrost-free watersheds (increasing as a function of watershed peatland coverage) than in permafrost-influenced watersheds. When combined with climate model simulations, these relationships enable a simple "space-for-time" substitution to estimate possible increases in N and P release from west Siberia by the year 2100. Results suggest that predicted climate warming in west Siberia will be associated with ~32–53% increases in DON concentrations, ~30–50% increases in TDN concentrations, and 29–47% increases in TDP concentrations as averaged across the region. While such increases in N and P are unlikely to significantly influence primary production in the Kara Sea as a whole, they will likely have large local impacts in the Ob' and Yenisey bays and nearshore environments.

**Citation:** Frey, K. E., J. W. McClelland, R. M. Holmes, and L. C. Smith (2007), Impacts of climate warming and permafrost thaw on the riverine transport of nitrogen and phosphorus to the Kara Sea, *J. Geophys. Res.*, 112, G04S58, doi:10.1029/2006JG000369.

### 1. Introduction

[2] Average annual arctic temperatures have increased at almost twice the global rate over recent decades and are predicted to increase by an additional 4–7°C over the next century [e.g., *Arctic Climate Impact Assessment*, 2005]. Continued warming will likely have profound consequences for many systems throughout the region, including permafrost extent [Lawrence and Slater, 2005], river discharge [Peterson et al., 2002; Manabe et al., 2004a, 2004b; Wu et al., 2005; Pavelsky and Smith, 2006; Smith et al., 2007] and stream biogeochemistry [e.g., Frey and Smith, 2005; Frey et al., 2007]. West Siberia (Figure 1) not only appears to be

particularly susceptible to changes in climate [Serreze et al., 2000; Frey and Smith, 2003], but it also plays a vital role in scenarios of arctic and global change because the region contains at least two key biophysical features, namely: (1) the presence of the world's most extensive organic-rich peatlands, where much of an estimated ~70 Pg of carbon is currently stored in permafrost [Sheng et al., 2004; Smith et al., 2004] and (2) the export of massive volumes of freshwater to the Kara Sea and Arctic Ocean, where the Ob' and Yenisey rivers of west Siberia alone supply ~35% of the total freshwater runoff that the Arctic Ocean receives [Aagaard and Carmack, 1989]. These two features in concert create a situation where the Kara Sea receives more dissolved organic matter (DOM) than any other part of the Arctic Ocean [Opsahl et al., 1999]. The Arctic Ocean in turn is an important global sink for terrestrial DOM, receiving more DOM per unit volume than any other ocean basin in the world [Opsahl et al., 1999]. Streams and rivers draining west Siberian peatlands thus provide a globally significant link between a massive pool of terrestrial organic matter and the adjacent marine environment.

<sup>1</sup>Graduate School of Geography, Clark University, Worcester, Massachusetts, USA.

<sup>2</sup>Marine Science Institute, University of Texas at Austin, Port Aransas, Texas, USA.

<sup>3</sup>Woods Hole Research Center, Falmouth, Massachusetts, USA.

<sup>4</sup>Department of Geography, University of California, Los Angeles, California, USA.

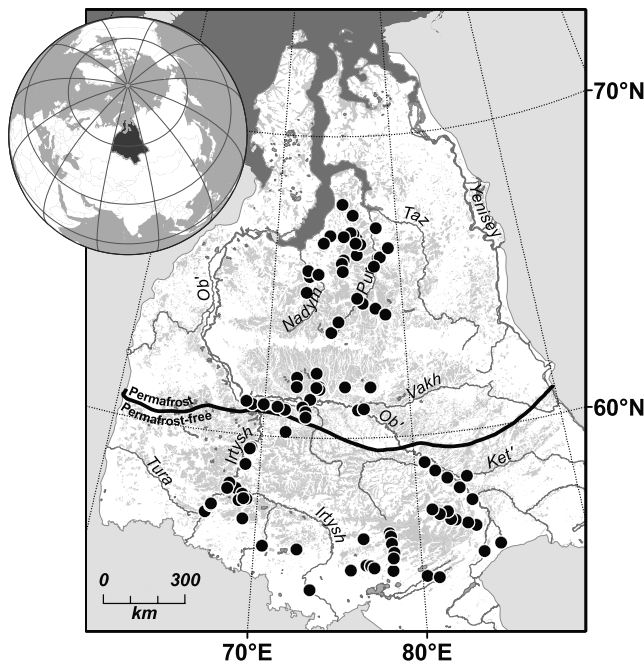


**Figure 1.** West Siberia and the locations of 96 water samples collected throughout the region. The permafrost limit, based on *Brown et al.* [1998], is also demarcated.

[3] Until recently, most water sampling campaigns in west Siberia have been constrained to the estuaries and main stems of the Ob'-Irtysh and Yenisey rivers [e.g., *Holmes et al.*, 2000, 2001; *Amon and Meon*, 2004]. However, new studies have presented both dissolved organic carbon (DOC) [*Frey and Smith*, 2005] and inorganic solutes [*Frey et al.*, 2007] in streams and rivers throughout the entire west Siberian region for a large range of watershed sizes, thus allowing for investigation of biogeochemical processes with higher spatial resolution. In this study, we present an unprecedented, comprehensive assessment of stream nitrogen and phosphorus (N and P) concentrations from sampling sites covering  $\sim 10^6$  km<sup>2</sup> throughout west Siberia. The samples span both permafrost-influenced and permafrost-free terrain, enabling speculation on how river-transported N and P may change under scenarios of continued climate warming in the region. These goals are achieved through presentation of dissolved organic nitrogen (DON), ammonium (NH<sub>4</sub>-N), nitrate (NO<sub>3</sub>-N), total dissolved nitrogen (TDN), and total dissolved phosphorus (TDP) concentrations from 96 streams and rivers located throughout west Siberia (Figure 1). Furthermore, we derive a regional hydrological model (similar to *Frey and Smith* [2005] and *Frey et al.* [2007]) in order to calculate summer-period (defined here as the months July–September) N and P fluxes from west Siberia. On the basis of these fluxes and climate model simulations for the next century, we predict the possible influence that climate warming may have on the riverine transport of N and P from west Siberia to the Kara Sea and adjacent Arctic Ocean by the year 2100.

## 2. Data and Methods

[4] West Siberia occupies  $\sim 2.6 \times 10^6$  km<sup>2</sup> and owing to its uniformly low topographic relief, is considered the

largest flat area on Earth [*Peterson and Clarke*, 1991]. Cool temperatures, poor drainage and waterlogged conditions have enabled accumulation of  $\sim 70$  Pg of carbon in the region's extensive peatlands over the last  $\sim 11,000$  annus [*Kremenetski et al.*, 2003; *Sheng et al.*, 2004; *Smith et al.*, 2004]. A recent and comprehensive inventory now confirms that the region contains nearly 600,000 km<sup>2</sup> of peatlands, representing a Holocene carbon sink of global significance [*Sheng et al.*, 2004; *Smith et al.*, 2004]. More than half of the region is influenced by permafrost ( $\sim 1.4 \times 10^6$  km<sup>2</sup> of its  $\sim 2.6 \times 10^6$  km<sup>2</sup> total land area), with  $\sim 15\%$  in continuous permafrost (northward of  $\sim 66^\circ\text{N}$ ) and  $\sim 39\%$  in discontinuous, sporadic or isolated patches of permafrost ( $\sim 61^\circ\text{N}$ – $66^\circ\text{N}$ ) (Figure 1). The two largest rivers draining west Siberia are the Ob' and Yenisey (Figure 1) with discharge of  $\sim 404$  km<sup>3</sup> a<sup>-1</sup> and  $\sim 620$  km<sup>3</sup> a<sup>-1</sup>, respectively [*Peterson et al.*, 2002].

[5] Sampling campaigns were undertaken from mid-July through late August of 1999, 2000 and 2001. Ninety-six spatially distributed water samples were collected from streams and rivers throughout the region, spanning a latitudinal gradient from  $\sim 55^\circ\text{N}$ – $68^\circ\text{N}$  over  $\sim 10^6$  km<sup>2</sup> (Figure 1). Sampled watersheds include 41 cold, permafrost-influenced and 55 warm, permafrost-free catchments, with drainage basin areas ranging from 37 km<sup>2</sup> to  $2.6 \times 10^6$  km<sup>2</sup>. Water samples were filtered in the field through Osmonics® 0.22 micron mixed esters membranes, stored in acid-washed high-density polyethylene bottles and refrigerated at 4°C until analyzed. NO<sub>3</sub>-N concentrations were determined by ion chromatography, whereas NH<sub>4</sub>-N, TDN and TDP concentrations were determined using a Perstorp Colorimetric Spectrophotometer. DON was calculated as the difference between TDN and (NO<sub>3</sub>-N + NH<sub>4</sub>-N). As TDP concentrations were based on dissolved components only, they do not take into account P associated with suspended sediments, which may be an important source of P in rivers [e.g., *Beusen et al.*, 2005]. All analyses were performed in the Department of Ecology and Systematics at Cornell University.

[6] Distinction between cold, permafrost-influenced and warm, permafrost free watersheds was established using the southern limit of permafrost as mapped by *Brown et al.* [1998]. Watershed areas were delineated with ESRI® ArcGIS™ v. 8.0 using Digital Chart of the World drainage networks, the GTOPO30 digital elevation model, U.S. Tactical Pilotage Charts, U.S. Operational Navigation Charts, and Russian Oblast maps. The percentage of peatland cover contained within each watershed was computed using a comprehensive GIS-based inventory of west Siberian peatlands [*Sheng et al.*, 2004]. MAAT was calculated for each watershed using gridded climate normals for years 1961–1990 [*New et al.*, 1999]. General circulation model (GCM) simulations, including the Geophysical Fluid Dynamics Laboratory R30, the Canadian Center for Climate Modeling and Analysis CGCM2, and the Max Planck Institute für Meteorologie ECHAM4 models were obtained from the IPCC Data Distribution Centre (<http://ipcc-ddc.cru.uea.ac.uk>). Model simulations were averaged over years 2071–2100. Map-based area calculations for all data were performed in the GIS using a Lambert Azimuthal Equal Area map projection.

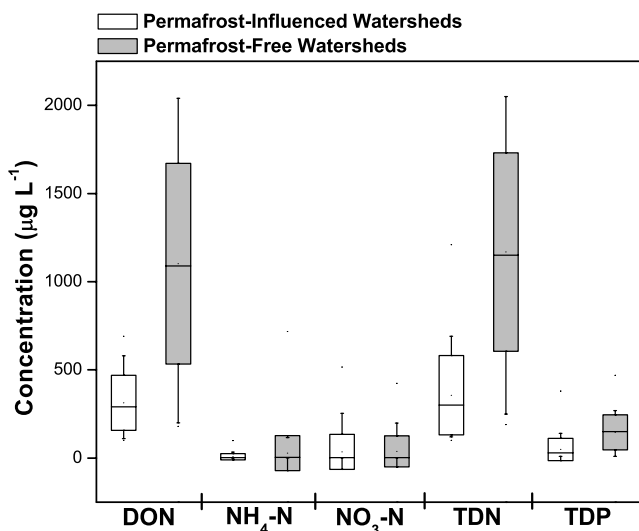


**Figure 2.** Concentrations of dissolved organic nitrogen (DON), ammonium (NH<sub>4</sub>-N), nitrate (NO<sub>3</sub>-N), total dissolved nitrogen (TDN) and total dissolved phosphorus (TDP) in all 96 permafrost-influenced and permafrost-free watersheds sampled throughout west Siberia. Mean values,  $\pm 1$  standard deviation (box), and confidence intervals of  $p < 0.05$  (whiskers) are shown. Two-sample t-Tests reveal that only concentrations of DON, TDN and TDP are statistically different from one another in permafrost-influenced versus permafrost-free watersheds (i.e.,  $p$  values are  $1.42 \times 10^{-13}$  (DON),  $0.20$  (NH<sub>4</sub>-N),  $0.89$  (NO<sub>3</sub>-N),  $9.11 \times 10^{-14}$  (TDN), and  $3.97 \times 10^{-7}$  (TDP)).

[7] Because arctic rivers display clear seasonal variations in N and P concentrations [Peterson *et al.*, 1992; Petrone *et al.*, 2006] (<http://ecosystems.mbl.edu/partners/>), we computed total N and P flux estimates for the summer period only, coincident with our sampling campaigns. These flux estimates were obtained by multiplying concentrations with modeled summer-period discharge for each watershed using the regression method of Mosley and McKerchar [1993], which is derived similarly to the annual discharge model of Frey and Smith [2005] and Frey *et al.* [2007]. This modeling approach was necessary for flux calculations, as sampling points rarely coincide with gauging stations. Here we utilized discharge ( $Q_s$ ), drainage area ( $A$ ) and watershed mean summer precipitation ( $P_s$ ) as input variables. In order to derive the regression equation,  $Q_s$ ,  $A$  and  $P_s$  were determined as follows: (1) 154 west Siberian gauging stations and associated summer period (July–September) discharge data (for years 1961–1990) were identified from the R-ArcticNET data network (<http://www.r-arcticnet.sr.unh.edu>); (2) watershed areas corresponding to each of the 154 gauging stations were delineated in a GIS just as for our 96 sampled watersheds (above); and (3) mean summer (July–September) precipitation over the watershed areas was determined in the GIS using gridded climate normals for years 1961–1990 [New *et al.*, 1999]. The resulting derived discharge estimation equation is as follows:

$$Q_s = 4.16 \times 10^{-20} \cdot A^{1.23} \cdot P_s^{6.13} (r^2 = 0.98), \quad (1)$$

where  $Q_s$  is total summer discharge (km<sup>3</sup>),  $A$  is drainage area (km<sup>2</sup>), and  $P_s$  is mean summer precipitation (mm). From this regression, the summer-period discharge at each of the 96 sample locations was calculated from their respective watershed areas and mean summer precipitation (see auxiliary material<sup>1</sup>). Although we cannot completely assume that July–September discharge is independent of stored precipitation from the previous winter, we chose to focus on the low-flow July–September period because it is after the spring flood that typically occurs in May or June in these west Siberian rivers. Corresponding N and P fluxes were then determined by multiplying summer discharge values by respective measured N and P concentrations at each of the sample locations. Because it is inappropriate to extrapolate summer-period N and P data to annual fluxes, we utilized this summer-period (July–September) approach as a first approximation in the absence of detailed flow-weighted data over the entire annual hydrograph in these remote locations. It is noteworthy, however, that when compared to the discharge estimation equation for annual discharge [Frey and Smith, 2005; Frey *et al.*, 2007], summer-period discharge (July–September) comprises (on average)  $\sim 33\%$  of the total annual discharge in streams and rivers throughout west Siberia.

### 3. Results

[8] The online auxiliary material presents N and P concentrations for all 96 watersheds sampled throughout west Siberia (including concentrations of DON, NH<sub>4</sub>-N, NO<sub>3</sub>-N, TDN and TDP). N and P concentrations range from 96–2506  $\mu\text{g L}^{-1}$  (DON), 0.5–718.2  $\mu\text{g L}^{-1}$  (NH<sub>4</sub>-N), 2.5–516.1  $\mu\text{g L}^{-1}$  (NO<sub>3</sub>-N), 99–2517  $\mu\text{g L}^{-1}$  (TDN), and 6–472  $\mu\text{g L}^{-1}$  (TDP). On average, TDN concentrations are approximately 8 times higher than those of TDP (821  $\mu\text{g L}^{-1}$  versus 104  $\mu\text{g L}^{-1}$ , respectively). Of the TDN species, DON constitutes the clear majority (with DON averaging 765  $\mu\text{g L}^{-1}$ , NH<sub>4</sub>-N averaging 19.3  $\mu\text{g L}^{-1}$ , and NO<sub>3</sub>-N averaging 36.7  $\mu\text{g L}^{-1}$  across all sampled watersheds). Furthermore, we observe significantly higher concentrations of DON, TDN and TDP in permafrost-free watersheds as compared to permafrost-influenced watersheds (Figure 2, Table 1, and auxiliary material). For permafrost-influenced and permafrost-free watersheds, respectively, DON averages 313 and 1103  $\mu\text{g L}^{-1}$ , TDN averages 355 and 1169  $\mu\text{g L}^{-1}$ , and TDP averages 48 and 146  $\mu\text{g L}^{-1}$  (Figure 2 and Table 1). However, the statistically significant difference in TDN concentrations between permafrost-influenced and permafrost-free watersheds (Table 1) is driven solely by DON: We find no statistically significant differences in concentrations of NH<sub>4</sub>-N, NO<sub>3</sub>-N between permafrost-influenced watersheds and permafrost-free watersheds (Figure 2 and Table 1).

[9] For those N and P species that do significantly differ between cold, permafrost-influenced and warm, permafrost-free watersheds (DON, TDN, and TDP), we note the following: DON and TDN (and TDP, to a lesser extent) concentrations exhibit a strong, positive linear correlation with DOC concentrations analyzed from the same stream

<sup>1</sup>Auxiliary materials are available at <ftp://ftp.agu.org/apend/jg/2006jg000369>.



**Table 1.** Concentrations and Summer-Period (July, August, and September) Fluxes of N and P Calculated for the West Siberian Region (Including Current Values and Those Predicted by the Year 2100)

	Concentration, $\mu\text{g L}^{-1}$					Summer Flux, $\times 10^9 \text{ g}$				
	DON	NH <sub>4</sub> -N	NO <sub>3</sub> -N	TDN	TDP	DON	NH <sub>4</sub> -N	NO <sub>3</sub> -N	TDN	TDP
All sites <sup>a</sup>	765	19.3	36.7	821	104	NA <sup>b</sup>	4.1	8.7	NA	NA
Permafrost-influenced <sup>c</sup>	313	7.6	35.1	355	48	NA	NA	NA	NA	NA
Permafrost-free <sup>c</sup>	1103	28.0	37.9	1169	146	NA	NA	NA	NA	NA
Total west Siberian region currently <sup>d</sup>	584	NA	NA	630	81	140	NA	NA	151	20
Total west Siberian region by 2100 (B2) <sup>d</sup>	770	NA	NA	820	104	185	NA	NA	197	25
Total west Siberian region by 2100 (A2) <sup>d</sup>	894	NA	NA	946	119	215	NA	NA	227	29

<sup>a</sup>Average values for all sites sampled. Average regional flux measurements for NH<sub>4</sub>-N and NO<sub>3</sub>-N were calculated by multiplying the average concentrations by the total regional summer (July, August, September) discharge value for west Siberia ( $\sim 240 \text{ km}^3$ ).

<sup>b</sup>Not applicable.

<sup>c</sup>Average concentrations for permafrost-influenced or permafrost-free watersheds (only DON, TDN and TDP are significantly different between the two permafrost regions).

<sup>d</sup>B2 (A2) calculation: corresponds to the most (least) conservative climate prediction in this study. Values for the total region calculated by linearly weighting permafrost-influenced and permafrost-free values by their respective areas (south or north of the  $-2^\circ\text{C}$  MAAT isotherm). These areas are dependent upon current surface air temperatures and future climate predictions for 2100 (Figure 6; see sections 3 and 4 for specific calculations). Regional fluxes were calculated by multiplying these concentrations by the total regional summer discharge value for west Siberia ( $\sim 240 \text{ km}^3$ ). Future estimates are made for DON, TDN, and TDP only.

and river water samples in west Siberia [Frey and Smith, 2005]. Concentrations of DON and TDN are approximately 3% those of DOC and concentrations of TDP are approximately 0.4% that of DOC (Figure 3). As such, the relationships of DON, TDN and TDP concentrations with permafrost influence, percent peatland cover, and watershed mean annual air temperature arise that are nearly identical to those for DOC [Frey and Smith, 2005]. Like DOC, the measured DON and TDN concentrations reveal a remarkable contrast between cold, permafrost-influenced and warm, permafrost-free watersheds (Figures 4 and 5). In permafrost-influenced watersheds, stream DON and TDN concentrations are uniformly low, regardless of the percentage of peatland cover within the watershed. In contrast, DON and TDN concentrations in permafrost-free watersheds rise rapidly as a function of peatland cover (Figure 4). Average DON concentrations in permafrost-free watersheds are more than triple those for permafrost-influenced watersheds ( $1103 \mu\text{g L}^{-1}$  versus  $313 \mu\text{g L}^{-1}$ ). Even higher contrasts are found in watersheds with extensive peatland cover (e.g., for watersheds with 80% peatland cover, DON is  $\sim 1682 \mu\text{g L}^{-1}$  versus  $\sim 313 \mu\text{g L}^{-1}$ ). The transition from low to high DON and TDN concentrations occurs at approximately the position of the  $-2^\circ\text{C}$  MAAT isotherm (Figure 5), which also coincides with the southern limit of permafrost (Figure 1). Therefore the  $-2^\circ\text{C}$  isotherm position and the permafrost limit together mark a critical threshold, south of which watershed DON and TDN concentrations begin rising quickly as a function of peatland cover. Although the relationships between TDP concentrations, percent peatland cover, and MAAT are weaker than those for DON and TDN (Figures 4 and 5), they are in fact statistically significant so we present and utilize these correlations in this study as well.

[10] Combining summer discharge estimates (as determined in section 2) and measured N and P concentrations (see auxiliary material), we calculate summer-period fluxes (in total summer g) for each of the sampled watersheds as a first estimate of the export of N and P from west Siberian streams and rivers (see auxiliary material). As these calculations incorporate a constant for summer discharge for each

of the sampled watersheds, these flux estimates do not reflect any interannual variability in discharge. For all sampled watersheds, N and P summer-period fluxes range from  $\sim 0-55288 \times 10^6 \text{ g}$  (DON),  $\sim 0-423 \times 10^6 \text{ g}$  (NH<sub>4</sub>-N),  $\sim 0-3193 \times 10^6 \text{ g}$  (NO<sub>3</sub>-N),  $\sim 0-55618 \times 10^6 \text{ g}$  (TDN), and  $\sim 0-6911 \times 10^6 \text{ g}$  (TDP) (see auxiliary material). Similar to N and P concentrations, there is a significant divergence in N and P fluxes between permafrost-influenced and permafrost-free watersheds (Table 1).

[11] A spatially averaged, regional concentration for each N and P species is averaged for the entire west Siberian region, following the approach of Frey and Smith [2005] for DOC and Frey *et al.* [2007] for inorganic solutes. Because NH<sub>4</sub>-N and NO<sub>3</sub>-N do not significantly differ between cold, permafrost-influenced watersheds and warm, permafrost-free watersheds, we simply average all samples to obtain a regionally averaged value ( $19.3 \mu\text{g L}^{-1}$  for NH<sub>4</sub>-N and  $36.7 \mu\text{g L}^{-1}$  for NO<sub>3</sub>-N) (Table 1). However, our regional estimates of stream DON, TDN and TDP concentrations are less straightforward and are based on the distribution of the land surface areas north and south of the  $-2^\circ\text{C}$  MAAT isotherm, the peatland coverage within these two temperature zones, and the empirical relationships between stream DON and watershed peatland cover established in Figure 4:

$$DON_{WPF} = 13.76 \cdot P_{\%} + 580; r = 0.56; p < 0.0001 \quad (2)$$

$$DON_{CPI} = 313(\text{constant}), \quad (3)$$

where  $DON_{WPF}$  is the DON concentration for warm, permafrost-free areas ( $\mu\text{g L}^{-1}$ );  $DON_{CPI}$  is the DON concentration for cold, permafrost-influenced areas ( $\mu\text{g L}^{-1}$ ); and  $P_{\%}$  is the percent of peatland cover of each watershed. Owing to the statistical insignificance of the DON- $P_{\%}$  relationship in cold, permafrost-influenced watersheds (Figure 4), we estimate  $DON_{CPI}$  as simply the mean concentration of those 41 samples ( $313 \mu\text{g L}^{-1}$ ). As TDN is strongly determined by DON concentrations (and also varies with percent peatland cover for permafrost-free

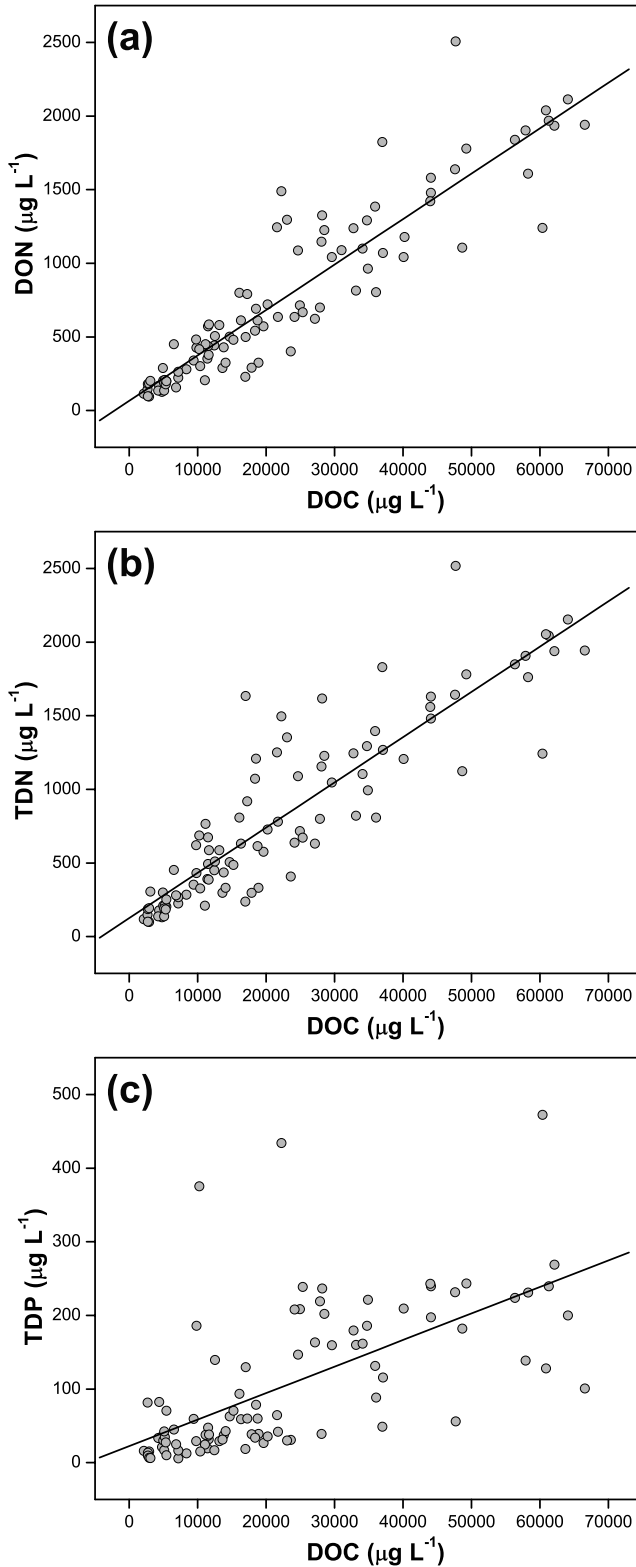


**Figure 3.** (a) DON, (b) TDN, and (c) TDP as a function of dissolved organic carbon (DOC). DON, TDN, and TDP concentrations are all significantly correlated with DOC concentrations (DON =  $0.03 \cdot \text{DOC} + 66$ ;  $p < 0.0001$ ;  $r = 0.92$ ); (TDN =  $0.03 \cdot \text{DOC} + 126$ ;  $p < 0.0001$ ;  $r = 0.89$ ); (TDP =  $0.004 \cdot \text{DOC} + 22$ ;  $p < 0.0001$ ;  $r = 0.64$ ).

watersheds), we employ a similar approach to obtain a regionally averaged TDN concentration, i.e.,

$$\text{TDN}_{WPF} = 14.82 \cdot P_{\%} + 606; r = 0.61; p < 0.0001 \quad (4)$$

$$\text{TDN}_{CPI} = 355(\text{constant}), \quad (5)$$

where  $\text{TDN}_{WPF}$  is the TDN concentration for warm, permafrost-free areas ( $\mu\text{g L}^{-1}$ ) and  $\text{TDN}_{CPI}$  is the TDN concentration for cold, permafrost-influenced areas ( $\mu\text{g L}^{-1}$ ). Lastly, we calculate the same for TDP:

$$\text{TDP}_{WPF} = 1.76 \cdot P_{\%} + 79; r = 0.40; p = 0.0022 \quad (6)$$

$$\text{TDP}_{CPI} = 48(\text{constant}), \quad (7)$$

where  $\text{TDP}_{WPF}$  is the TDP concentration for warm, permafrost-free areas ( $\mu\text{g L}^{-1}$ ) and  $\text{TDP}_{CPI}$  is the TDP concentration for cold, permafrost-influenced areas ( $\mu\text{g L}^{-1}$ ).

[12] Once established, these relationships may be multiplied by the total land-surface areas north and south of the  $-2^{\circ}\text{C}$  MAAT isotherm in west Siberia to calculate regionally averaged concentrations for all of west Siberia. Of the total area ( $\sim 2.63 \times 10^6 \text{ km}^2$ ),  $\sim 52\%$  ( $\sim 1.37 \times 10^6 \text{ km}^2$ ) currently lies north of the  $-2^{\circ}\text{C}$  MAAT isotherm and  $48\%$  ( $\sim 1.26 \times 10^6 \text{ km}^2$ ) lies south. A simple linear mixing model that weights equations (2)–(7) by these land-area proportions is

$$X_{\text{current}} = (0.52 \cdot X_{CPI}) + (0.48 \cdot X_{WPF}), \quad (8)$$

where  $X_{\text{current}}$  ( $\mu\text{g L}^{-1}$ ) is the current regionally averaged concentration of DON, TDN or TDP available for export from the west Siberian region.  $X_{CPI}$  and  $X_{WPF}$  ( $\mu\text{g L}^{-1}$ ) are the cold, permafrost-influenced and warm, permafrost-free concentrations of DON, TDN and TDP from equations (2)–(7), above. Equation (8) thus yields concentrations currently available for export (as averaged over the entire west Siberian land surface; Figure 1) of  $\sim 584 \mu\text{g L}^{-1}$  for DON,  $630 \mu\text{g L}^{-1}$  for TDN, and  $81 \mu\text{g L}^{-1}$  for TDP (Table 1).

[13] To calculate regional summer-period N and P fluxes from west Siberia, equation (1) is used to determine a regionally averaged summer-period discharge estimate of  $\sim 240 \text{ km}^3$  for the entire west Siberian region ( $A \sim 2.63 \times 10^6 \text{ km}^2$ ;  $P_s \sim 182 \text{ mm}$ ). Next, regional DON,  $\text{NH}_4\text{-N}$ ,  $\text{NO}_3\text{-N}$ , TDN and TDP fluxes are computed by multiplying this discharge with the concentrations in Table 1, yielding  $\sim 140 \times 10^9 \text{ g}$  (DON),  $\sim 4.1 \times 10^9 \text{ g}$  ( $\text{NH}_4\text{-N}$ ),  $\sim 8.7 \times 10^9 \text{ g}$  ( $\text{NO}_3\text{-N}$ ),  $\sim 151 \times 10^9 \text{ g}$  (TDN), and  $\sim 20 \times 10^9 \text{ g}$  (TDP) (Table 1). Again, as these calculations incorporate a constant for summer discharge, these flux estimates do not reflect any interannual variability in discharge. Furthermore, implicit in these flux calculations is the assumption that N and P concentrations do not vary between July and September.

#### 4. Discussion

[14] Our results show that the  $-2^{\circ}\text{C}$  MAAT isotherm and/or the permafrost limit in west Siberia mark a clear

threshold, with cold, permafrost-influenced watersheds exhibiting low DON, TDN and TDP concentrations and warm, permafrost-free watersheds exhibiting significantly higher DON, TDN and TDP concentrations (Figure 2, Table 1, and auxiliary material). Because  $\sim 52\%$  ( $\sim 1.37 \times 10^6 \text{ km}^2$ ) of the west Siberian land surface is currently north of that

limit, continued arctic climate warming may ultimately lead to increased release of N and P to the Kara Sea and Arctic Ocean as it migrates northward. On the basis of our measured concentrations, we estimate that the current regionally averaged N and P summer-period concentrations over the entire west Siberian region ( $\sim 2.6 \times 10^6 \text{ km}^2$ ) are  $\sim 584$ ,  $\sim 630$ , and  $81 \mu\text{g L}^{-1}$  (with summer-period fluxes of  $\sim 140 \times 10^9$ ,  $\sim 150 \times 10^9$ , and  $\sim 20 \times 10^9 \text{ g}$ ) for DON, TDN and TDP, respectively. Depending on the model used, GCM simulations predict that the total land area in west Siberia south of the  $-2^\circ\text{C}$  MAAT isotherm will increase to  $\sim 2.0\text{--}2.6 \times 10^6 \text{ km}^2$  ( $\sim 75\text{--}98\%$  of the total west Siberian area) by 2100 (Figure 6). Modification of equation (8) to reflect these climate change scenarios yields

$$X_{B2} = (0.25 \cdot X_{CPI}) + (0.75 \cdot X_{WPF}) \quad (9)$$

$$X_{A2} = (0.02 \cdot X_{CPI}) + (0.98 \cdot X_{WPF}), \quad (10)$$

where  $X_{B2}$  ( $\mu\text{g L}^{-1}$ ) is the regionally averaged N or P concentration available for export in 2100 using the most conservative climate prediction (B2 scenario of CGCM2) and  $X_{A2}$  ( $\mu\text{g L}^{-1}$ ) is that for the least conservative climate prediction in 2100 (A2 scenario of ECHAM4). Assuming no changes in summer-period discharge, equations (9) and (10) yield projected N and P concentrations available for export from the entire west Siberian region of  $\sim 770\text{--}894 \mu\text{g L}^{-1}$  (DON),  $\sim 820\text{--}946 \mu\text{g L}^{-1}$  (TDN), and  $\sim 122\text{--}143 \mu\text{g L}^{-1}$  (TDP) by the year 2100 (Table 1). Such values would represent a 32–53% increase in DON, a 30–50% increase in TDN, and a 28–47% increase in TDP concentrations. Summer-period fluxes to the Kara Sea are projected to increase to  $\sim 185\text{--}215 \times 10^9 \text{ g}$  for DON (+32–53%),  $\sim 197\text{--}227 \times 10^9 \text{ g}$  for TDN (+30–50%), and  $\sim 25\text{--}29 \times 10^9 \text{ g}$  for TDP (+28–47%) (Table 1). It is important to note that all such flux projections depend on river discharge and therefore will be altered by changes in river runoff [e.g., *Berezovskaya et al.*, 2004; *McClelland et al.*, 2004; *Yang et al.*, 2004a, 2004b; *Ye et al.*, 2004; *Wu et al.*, 2005]. However, if recently observed increases in west Siberian precipitation [*Frey and Smith*, 2003] continue and model predictions of increased river discharge in this next century do come to pass [*Peterson et al.*, 2002; *Manabe et al.*, 2004a, 2004b; *Wu et al.*, 2005], the true summer-period export of N and P will be even larger. This may be even further enhanced owing to observed positive correlations between DOM concentrations and discharge [*Peterson et al.*, 1992; *Finlay et al.*, 2006; *Petrone et al.*, 2006]. Thus the

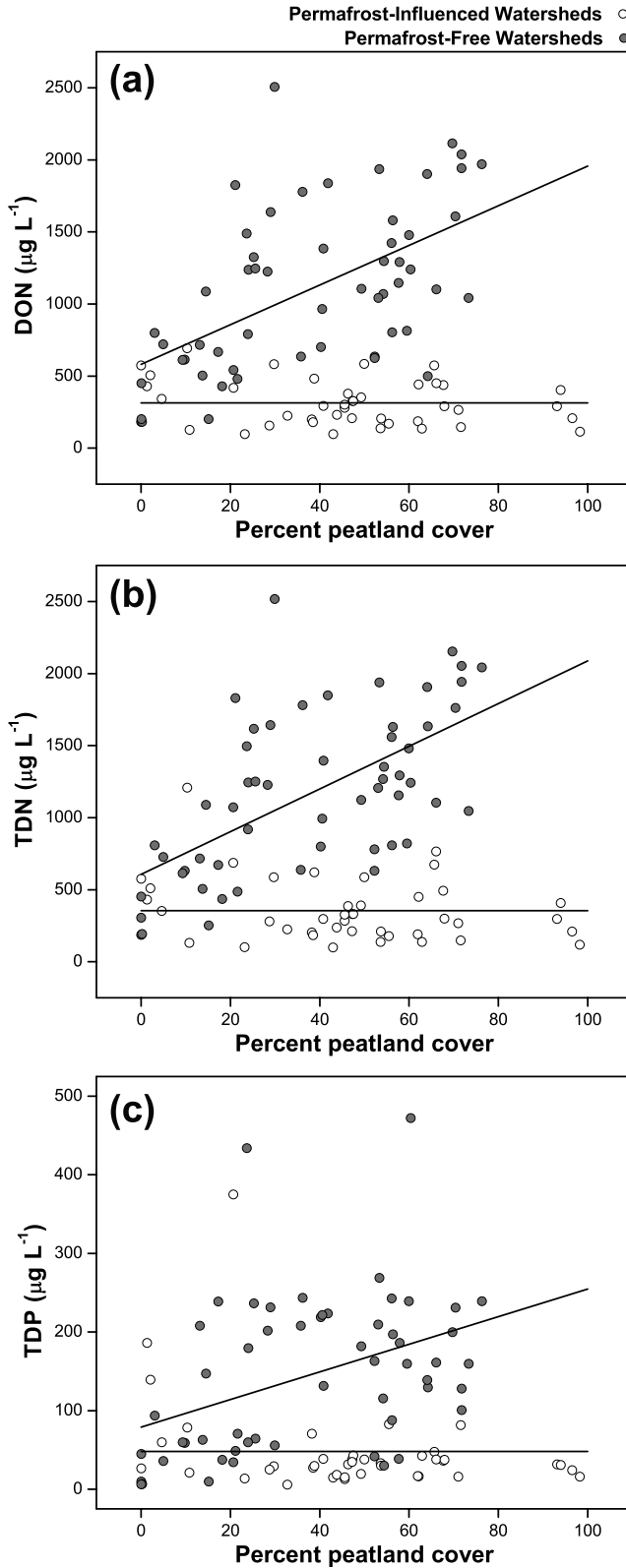


**Figure 4.** Dependence of (a) DON, (b) TDN, and (c) TDP concentrations on the percent peatland cover ( $P_{\%}$ ) within the sampled watersheds. N and P concentrations in permafrost-influenced watersheds are uniformly low, with mean values of  $313 \mu\text{g L}^{-1}$  (DON),  $355 \mu\text{g L}^{-1}$  (TDN), and  $48 \mu\text{g L}^{-1}$  (TDP) and no statistically significant correlation with  $P_{\%}$ . However, N and P concentrations in permafrost-free watersheds rise significantly with  $P_{\%}$  ( $\text{DON} = 13.76 \cdot P_{\%} + 580$ ;  $p < 0.0001$ ;  $r = 0.56$ ); ( $\text{TDN} = 14.82 \cdot P_{\%} + 606$ ;  $p < 0.0001$ ;  $r = 0.61$ ); ( $\text{TDP} = 1.76 \cdot P_{\%} + 79$ ;  $p < 0.0001$ ;  $r = 0.40$ ).

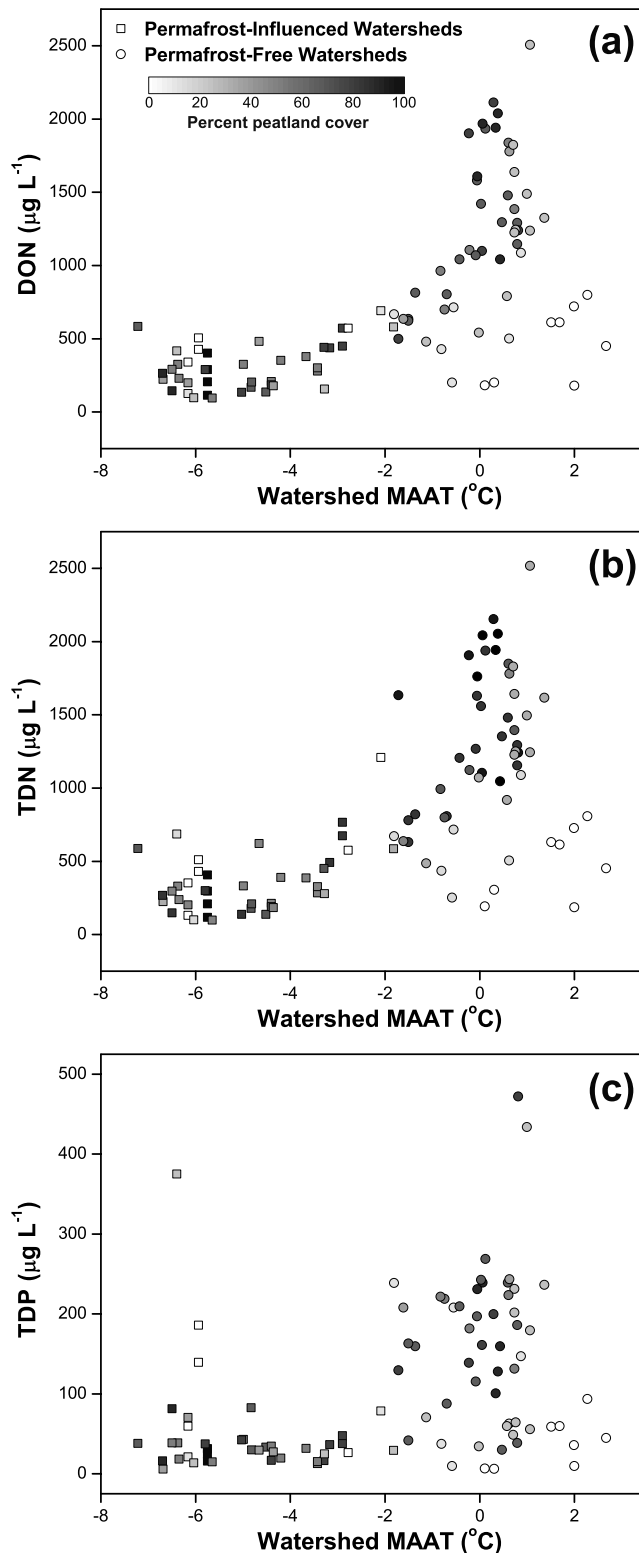


**Figure 5.** Dependence of (a) DON, (b) TDN, and (c) TDP concentrations on watershed mean annual air temperature (MAAT). A sharp increase in concentrations occurs in watersheds with a MAAT warmer than  $-2^{\circ}\text{C}$ . Low concentrations in permafrost-free watersheds are primarily due to sparse peatland coverage.

above projections of summer-period export of DON, TDN and TDP are likely conservative. Furthermore, as modern northern peatlands cover  $\sim 4 \times 10^6 \text{ km}^2$  [MacDonald *et al.*, 2006] with much of this area currently influenced by permafrost, similar increases in N and P export from rivers throughout the circumarctic region to the Arctic Ocean are likely over the coming century.

[15] Increased loads of C [e.g., Frey and Smith, 2005], N and P, combined with warmer water temperatures, are likely to lead to a general increase in total productivity within arctic streams and rivers [Prowse *et al.*, 2006]. Currently, inorganic N and P concentrations are quite low and limiting in arctic rivers [Holmes *et al.*, 2000, 2001], therefore any increase in inorganic N and P should stimulate production [e.g., Peterson *et al.*, 1993; Flanagan *et al.*, 2003]. Although we do not predict significant increases in concentrations of inorganic N species ( $\text{NH}_4\text{-N}$  and  $\text{NO}_3\text{-N}$ ) in west Siberian streams with warming and permafrost thaw, our predicted increases in DON loads could still have important implications for stimulating production within these watersheds [Neff *et al.*, 2003]. However, decomposition rates of in-stream DOM can be relatively slow compared to watershed transit times [Striegl *et al.*, 2007], suggesting that only a small portion of the DON load may be mineralized before reaching the marine environment and resulting impacts on in-stream production would thus be minimal. Increased export of DOM through west Siberian streams and rivers may therefore be more important for production in the adjacent marine environment.

[16] Estimates of primary production in the Kara Sea as a whole ( $\sim 926,000 \text{ km}^2$ ) range from  $13.5 \times 10^6$  to  $41.7 \times 10^6 \text{ tons C a}^{-1}$  [Gebhardt *et al.*, 2005]. We use a conser-

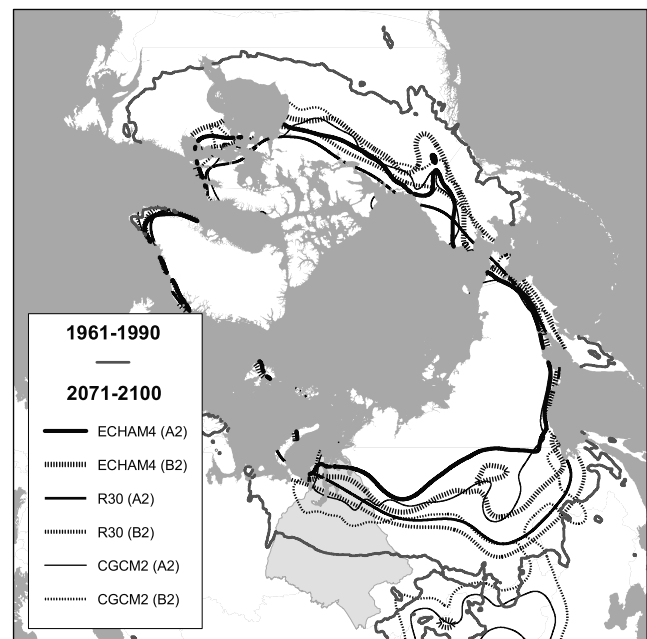


**Figure 6.** Locations of  $-2^{\circ}\text{C}$  MAAT isotherms, based on observational data from 1961–1990 [New *et al.*, 1999] and modeled data from 2071–2100 (using the R30, CGCM2, and ECHAM4 models). Both the A2 (less conservative) and B2 (more conservative) IPCC greenhouse gas emission scenarios are shown for each model.



vative midpoint of  $20 \times 10^6$  tons  $C\ a^{-1}$  [Vinogradov *et al.*, 2000] as a reference point for comparison with N exports from west Siberia. Assuming Redfield stoichiometry,  $20 \times 10^6$  tons  $C\ a^{-1}$  of primary production represents a N demand of  $\sim 3.0 \times 10^6$  tons  $N\ a^{-1}$ . Summer inputs of TDN from the west Siberian region currently amount to about 5% of this demand. Thus increasing summer N export from west Siberia by 30–50% (Table 1) would have little effect on overall primary production in the Kara Sea. However, the outlook is quite different for the nearshore environment where riverine waters are most concentrated. For the Ob' and Yenisey bays and nearshore waters to  $74^\circ N$  ( $\sim 70,000\ km^2$ ), we calculate that N demand is  $\sim 0.23 \times 10^6$  tons  $N\ a^{-1}$  and  $\sim 0.17 \times 10^6$  tons N during the summer period (July–September). The latter value is comparable to a N demand of  $0.12 \times 10^6$  tons N during the summer period, which we calculate on the basis of primary production measurements collected during the 49th cruise of the R/V *Dmitriy Mendeleev* in September 1993 [Vedernikov *et al.*, 1995]. Thus summer N export from the west Siberian region (Table 1) amounts to approximately 90–125% of the summer N demand in nearshore waters. Given these high percentages, projected increases in summer N export from west Siberia (Table 1) have the potential to substantially influence primary production in the nearshore Kara Sea.

[17] Given that most of the projected change in TDN export is accounted for by a change in DON export, the lability of this material and the amount of N that may be remineralized during processing must also be considered. It has been traditionally thought that DON is largely refractory and unimportant to marine primary productivity; however, recent work has shown that recycling of nitrogen through the DON pool can be large and important for phytoplankton nutrition [Bronk *et al.*, 2006]. Thus, while we may not expect significant impacts on in-stream production nor significant increases in riverine inorganic N export over the coming century, our predicted increases in DON delivery to the Kara Sea may in fact have significant consequences for primary production in the adjacent marine environment. Although it is difficult to predict the lability of the DON that would be liberated as a consequence of warming and permafrost thaw, new evidence suggests that such DOM may be more labile than previously thought: Until recently, DOM exported from arctic rivers was considered to be largely recalcitrant [Opsahl *et al.*, 1999; Dittmar and Kattner, 2003; Rachold *et al.*, 2003; Amon and Meon, 2004], but new evidence suggests that  $\sim 30\%$  may be rapidly processed in the nearshore environment [Cooper *et al.*, 2005]. This, of course, has implications for utilization of river-borne TDP in coastal waters as well. However, changes in TDP export from rivers are not expected to have a significant impact on coastal productivity as long as N demand limits primary production.

[18] The major increases in DON export and the lack of changes in dissolved inorganic N ( $NO_3-N$  and  $NH_4-N$ ) export predicted here contrast with findings from a recent study of long-term data from the upper Kuparuk River, North Slope, Alaska [McClelland *et al.*, 2007]. In that study, major increases in  $NO_3-N$  export were identified during recent years (associated with increasing ground temperatures), but with little change in DOM. The apparent difference between the two studies may reflect a difference

in the timing of sampling: The Kuparuk samples were in fact collected May–August with changes most pronounced during the spring freshet. There may also exist regional differences in ecosystem responses: In the Alaskan interior, Petrone *et al.* [2006] found significantly lower exports of DOM and significantly higher exports of  $NO_3-N$  from permafrost-free watersheds as compared to permafrost-influenced watersheds. However, it may be difficult to compare space-for-time substitutions with time series studies because the former consider ecosystems at different steady (or quasisteady) states whereas the latter captures transitional dynamics.

[19] A variety of mechanisms may account for the observed differences in dissolved organic N and P concentrations between cold, permafrost-influenced watersheds and warm, permafrost-free watersheds. First, dissolved organic N and P increases may be driven by warmer air temperatures, through temperature-related processes of DOM production: Warming may increase peat decomposition and thus DOM production by enhancing microbial respiration [e.g., Christ and David, 1996; Freeman *et al.*, 2001]. Furthermore, warming may enhance photosynthesis and aboveground plant biomass, thereby increasing DOM production by providing a larger source pool of organic matter [e.g., Moore *et al.*, 1998]. In many cases, increased adsorption of DOM may in fact decrease exports in areas where permafrost thaw leads to greater flow through mineral soils [e.g., MacLean *et al.*, 1999; Moore and Turunen, 2004; Petrone *et al.*, 2006]. However because mineral soils are overlain by  $\sim 1$ – $5$  m of peat in west Siberia [Sheng *et al.*, 2004], increased DOM adsorption by mineral soils would be limited and thus DOM export would be maximized. Second, in permafrost areas, hydrologic transport of DOM from peatlands to their outlet streams may be limited by the presence of ice-rich permafrost. Although northern soils most commonly export recently fixed carbon of plant and near-surface soil origin [Benner *et al.*, 2004] (suggesting little hydrologic interaction at depth), radiocarbon dating has also shown riverine DOM to be much older than previously thought [Raymond and Bauer, 2001] (suggesting that base flow from older, deeper peats may also export DOM to streams). If relatively deep peat soils are a source of DOM to streams and rivers, ice-rich permafrost may in fact present a physical barrier to infiltration and subsurface flow through peatlands in the northern half of west Siberia (thus confining the process of DOM production and hydrologic transport to the shallow surface active layer and effectively eliminating large depths of organic-rich peat ( $\sim 1$ – $5$  m) [Sheng *et al.*, 2004] as a source of DOM). Thus the degradation of permafrost in peatlands may amplify DOM export to streams, which again, could partly depend upon the sorption ability of newly thawed subpeat soils [MacLean *et al.*, 1999; Moore and Turunen, 2004; Petrone *et al.*, 2006].

## 5. Conclusions and Implications

[20] Previous studies have shown the potential for increased export of both DOC [Frey and Smith, 2005] and inorganic solutes [Frey *et al.*, 2007] from west Siberia to the Kara Sea in response to GCM predictions of climate warming in the 21st century. Here we project comparable



increases in DON, TDN and TDP export as well. However, unlike DON, TDN, TDP, DOC and inorganic solutes, we find no significant contrast in concentrations of inorganic N species ( $\text{NH}_4\text{-N}$  and  $\text{NO}_3\text{-N}$ ) between cold, permafrost-influenced watersheds and warm, permafrost-free watersheds. Instead, significant contrasts are found for DON, TDN and TDP with uniformly low concentrations in cold, permafrost-influenced watersheds but higher concentrations in warm, permafrost-free watersheds, rising sharply as a function of peatland cover. The two regimes appear to be separated by the geographic position of the  $-2^\circ\text{C}$  MAAT isotherm, which is also approximately coincident with the permafrost limit. Climate model simulations for the next century predict near-doubling of west Siberian land surface areas with a MAAT warmer than  $-2^\circ\text{C}$ , suggesting  $\sim 32\text{--}53\%$  increases in DON concentrations,  $\sim 30\text{--}50\%$  increases in TDN concentrations, and  $29\text{--}47\%$  increases in TDP concentrations as averaged across the entire west Siberian region. For the summer period (July–September) only, these increases in concentrations translate to a  $45\text{--}75 \times 10^9$  g increase in DON flux,  $46\text{--}76 \times 10^9$  g increase in TDN flux, and  $5\text{--}9 \times 10^9$  g increase in TDP flux. While such increases are unlikely to impact biological productivity for in-stream processes nor the Kara Sea as a whole, they are expected to significantly increase primary production in the Ob' and Yenisey bays and nearshore environments.

[21] **Acknowledgments.** Funding for this research was provided by the NSF Arctic System Science Program (ARCSS) Freshwater Initiative (ARC-023091). Additional funding was provided by the NSF ARCS Program through the Russian-American Initiative on Shelf-Land Environments of the Arctic (OPP-9818496) and NASA through an Earth System Science Fellowship (NGT5-30338). We thank A. Velichko, G. MacDonald, O. Borisova, and K. Kremenetski for their logistical and scientific assistance in the field and M. Brown at Cornell University for performing water sample analyses. We additionally wish to thank two anonymous reviewers for their constructive comments and suggestions.

## References

- Aagaard, K., and E. C. Carmack (1989), The role of sea ice and other fresh water in the Arctic circulation, *J. Geophys. Res.*, **94**, 14,485–14,498.
- Amon, R. M. W., and B. Meon (2004), The biogeochemistry of dissolved organic matter and nutrients in two large Arctic estuaries and potential implications for our understanding of the Arctic Ocean system, *Mar. Chem.*, **92**, 311–330.
- Arctic Climate Impact Assessment (2005), *Arctic Climate Impact Assessment*, 1042 pp., Cambridge Univ. Press, New York. (Available at <http://www.acia.uaf.edu>)
- Benner, R., B. Benitez-Nelson, K. Kaiser, and R. M. W. Amon (2004), Export of young terrigenous dissolved organic carbon from rivers to the Arctic Ocean, *Geophys. Res. Lett.*, **31**, L05305, doi:10.1029/2003GL019251.
- Berezovskaya, S., D. Yang, and D. L. Kane (2004), Compatibility analysis of precipitation and runoff trends over the large Siberian watersheds, *Geophys. Res. Lett.*, **31**, L21502, doi:10.1029/2004GL021277.
- Beusen, A. H. W., A. L. M. Dekkers, A. F. Bouwman, W. Ludwig, and J. Harrison (2005), Estimation of global river transport of sediments and associated particulate C, N, and P, *Global Biogeochem. Cycles*, **19**, GB4S05, doi:10.1029/2005GB002453.
- Bronk, D. A., J. J. See, P. Bradley, and L. Killberg (2006), DON as a source of bioavailable nitrogen for phytoplankton, *Biogeosci. Discuss.*, **3**, 1247–1277.
- Brown, J., O. J. Ferrians Jr., J. A. Heginbottom, and E. S. Melnikov (1998), Circumarctic map of permafrost and ground-ice conditions, report, Natl. Snow and Ice Data Cent., World Data Cent. for Glaciol., Boulder, Colo.
- Christ, M. J., and M. B. David (1996), Temperature and moisture effects on the production of dissolved organic carbon in a spodosol, *Soil Biol. Biochem.*, **28**, 1191–1199.
- Cooper, L. W., R. Benner, J. W. McClelland, B. J. Peterson, R. M. Holmes, P. A. Raymond, D. A. Hansell, J. M. Grebmeier, and L. A. Codispoti (2005), Linkages among runoff, dissolved organic carbon, and the stable isotope composition of seawater and other water mass indicators in the Arctic Ocean, *J. Geophys. Res.*, **110**, G02013, doi:10.1029/2005JG000031.
- Dittmar, T., and G. Kattner (2003), The biogeochemistry of the river and shelf ecosystem of the Arctic Ocean: A review, *Mar. Chem.*, **83**, 103–120.
- Finlay, J., J. Neff, S. Zimov, A. Davydova, and S. Davydov (2006), Snow-melt dominance of dissolved organic carbon in high-latitude watersheds: Implications for characterization and flux of river DOC, *Geophys. Res. Lett.*, **33**, L10401, doi:10.1029/2006GL025754.
- Flanagan, K. M., E. McMauley, F. Wrona, and T. Prowse (2003), Climate change: The potential for latitudinal effects on algal biomass in aquatic ecosystems, *Can. J. Fish. Aquat. Sci.*, **60**, 635–639.
- Freeman, C., C. D. Evans, and D. T. Monteith (2001), Export of organic carbon from peat soils, *Nature*, **412**, 785.
- Frey, K. E., and L. C. Smith (2003), Recent temperature and precipitation increases in west Siberia and their association with the Arctic Oscillation, *Polar Res.*, **22**, 287–300.
- Frey, K. E., and L. C. Smith (2005), Amplified carbon release from vast west Siberian peatlands by 2100, *Geophys. Res. Lett.*, **32**, L09401, doi:10.1029/2004GL020225.
- Frey, K. E., D. I. Siegel, and L. C. Smith (2007), Geochemistry of west Siberian streams and their potential response to permafrost degradation, *Water Resour. Res.*, **43**, W03406, doi:10.1029/2006WR004902.
- Gebhardt, A. C., B. Gaye-Haake, D. Unger, N. Lahajnar, and V. Ittekkot (2005), A contemporary sediment and organic carbon budget for the Kara Sea shelf (Siberia), *Mar. Geol.*, **220**, 83–100.
- Holmes, R. M., B. J. Peterson, V. V. Gordeev, A. V. Zhulidov, M. Meybeck, R. B. Lammers, and C. J. Vörösmarty (2000), Flux of nutrients from Russian rivers to the Arctic Ocean: Can we establish a baseline against which to judge future changes?, *Water Resour. Res.*, **36**, 2309–2320.
- Holmes, R. M., B. J. Peterson, A. V. Zhulidov, V. V. Gordeev, P. N. Makkaveev, P. A. Stunzhas, L. S. Kosmenko, G. H. Kohler, and A. I. Shiklomanov (2001), Nutrient chemistry of the Ob' and Yenisey Rivers, Siberia: results from June 2000 expedition and evaluation of long-term data sets, *Mar. Chem.*, **75**, 219–227.
- Kremenetski, K. V., A. A. Velichko, O. K. Borisova, G. M. MacDonald, L. C. Smith, K. E. Frey, and L. A. Orlova (2003), Peatlands of the western Siberian lowlands: Current knowledge on zonation, carbon content and late Quaternary history, *Quat. Sci. Rev.*, **22**, 703–723.
- Lawrence, D. M., and A. G. Slater (2005), A projection of near-surface permafrost degradation during the 21st century, *Geophys. Res. Lett.*, **32**, L24401, doi:10.1029/2005GL025080.
- MacDonald, G. M., D. W. Beilman, K. V. Kremenetski, Y. Sheng, L. C. Smith, and A. A. Velichko (2006), Rapid early development of circumarctic peatlands and atmospheric  $\text{CH}_4$  and  $\text{CO}_2$  variations, *Science*, **314**, 285–288.
- MacLean, R., M. W. Oswood, J. G. Irons III, and W. H. McDowell (1999), The effect of permafrost on stream biogeochemistry: A case study of two streams in the Alaskan (U.S.A) taiga, *Biogeochemistry*, **47**, 239–267.
- Manabe, S., P. C. D. Milly, and R. Wetherald (2004a), Simulated long-term changes in river discharge and soil moisture due to global warming, *Hydrol. Sci. J.*, **49**, 625–642.
- Manabe, S., R. T. Wetherald, P. C. D. Milly, T. L. Delworth, and R. J. Stouffer (2004b), Century-scale change in water availability:  $\text{CO}_2$ -quadrupling experiment, *Clim. Change*, **64**, 59–76.
- McClelland, J. W., R. M. Holmes, B. J. Peterson, and M. Stieglitz (2004), Increasing river discharge in the Eurasian Arctic: Consideration of dams, permafrost thaw, and fires as potential agents of change, *J. Geophys. Res.*, **109**, D18102, doi:10.1029/2004JD004583.
- McClelland, J. W., M. Stieglitz, F. Pan, R. M. Holmes, and B. J. Peterson (2007), Recent changes in nitrate and dissolved organic carbon export from the upper Kuparuk River, North Slope, Alaska, *J. Geophys. Res.*, doi:10.1029/2006JG000371, in press.
- Moore, T. R., and J. Turunen (2004), Carbon accumulation and storage in mineral soil beneath peat, *Soil Sci. Soc. Am. J.*, **68**, 690–696.
- Moore, T. R., N. T. Roulet, and J. M. Waddington (1998), Uncertainty in predicting the effect of climatic change on the carbon cycling of Canadian peatlands, *Clim. Change*, **40**, 229–245.
- Mosley, M. P., and A. I. McKerchar (1993), Streamflow, in *Handbook of Hydrology*, edited by D. R. Maidment, pp. 8.1–8.39, McGraw-Hill, New York.
- Neff, J. C., F. S. Chapin III, and P. M. Vitousek (2003), Breaks in the cycle: Dissolved organic nitrogen in terrestrial ecosystems, *Front. Ecol. Environ.*, **1**, 205–211.
- New, M., M. Hulme, and P. Jones (1999), Representing twentieth-century space-time climate variability. Part I: Development of a 1961–90 mean monthly terrestrial climatology, *J. Clim.*, **12**, 829–856.
- Opsahl, S., R. Benner, and R. W. Amon (1999), Major flux of terrigenous dissolved organic matter through the Arctic Ocean, *Limnol. Oceanogr.*, **44**, 2017–2023.

- Pavelsky, T. M., and L. C. Smith (2006), Intercomparison of four global precipitation datasets and their correlation with increased Eurasian river discharge to the Arctic Ocean, *J. Geophys. Res.*, *111*, D21112, doi:10.1029/2006JD007230.
- Peterson, B. J., T. Corliss, K. Kriet, and J. E. Hobbie (1992), Nitrogen and phosphorus concentrations and export for the upper Kuparuk River on the North Slope of Alaska, *Hydrobiologia*, *240*, 61–69.
- Peterson, B. J., et al. (1993), Biological responses of a tundra river to fertilization, *Ecology*, *74*, 653–672.
- Peterson, B. J., R. M. Holmes, J. W. McClelland, C. J. Vörösmarty, R. B. Lammers, A. I. Shiklomanov, I. A. Shiklomanov, and S. Rahmstorf (2002), Increasing river discharge to the Arctic Ocean, *Science*, *298*, 2171–2173.
- Peterson, J. A., and J. W. Clarke (1991), *Geology Hydrocarbon Habitat of the West Siberian Basin*, 96 pp., Am. Assoc. of Pet. Geol. Tulsa, Okla.
- Petrone, K. C., J. B. Jones, L. D. Hinzman, and R. D. Boone (2006), Seasonal export of carbon, nitrogen, and major solutes from Alaskan catchments with discontinuous permafrost, *J. Geophys. Res.*, *111*, G02020, doi:10.1029/2005JG000055.
- Prowse, T. D., F. J. Wrona, J. D. Reist, J. J. Gibson, J. E. Hobbie, L. M. J. Lévesque, and W. F. Vincent (2006), Climate change effects on hydroecology of arctic freshwater ecosystems, *Ambio*, *35*, 347–358.
- Rachold, V., H. Eiken, V. V. Gordeev, M. N. Grigoriev, H. W. Hubberten, A. P. Lisitzin, V. P. Shevchenko, and L. Schirrmeister (2003), Modern terrigenous organic carbon input to the Arctic Ocean, in *The Organic Carbon Cycle in the Arctic Ocean*, edited by R. Stein and R. W. Macdonald, pp. 33–55, Springer, Berlin.
- Raymond, P. A., and J. E. Bauer (2001), Riverine export of aged terrestrial organic matter to the North Atlantic Ocean, *Nature*, *409*, 497–500.
- Serreze, M. C., J. E. Walsh, F. S. Chapin III, T. Osterkamp, M. Dyurgerov, V. Romanovsky, W. C. Oechel, J. Morison, T. Zhang, and R. G. Barry (2000), Observational evidence of recent change in the northern high-latitude environment, *Clim. Change*, *46*, 159–207.
- Sheng, Y., L. C. Smith, G. M. MacDonald, K. V. Kremenetski, K. E. Frey, A. A. Velichko, M. Lee, D. W. Beilman, and P. Dubinin (2004), A high-resolution GIS-based inventory of the west Siberian peat carbon pool, *Global Biogeochem. Cycles*, *18*, GB3004, doi:10.1029/2003GB002190.
- Smith, L. C., G. M. MacDonald, A. A. Velichko, D. W. Beilman, O. K. Borisova, K. E. Frey, K. V. Kremenetski, and Y. Sheng (2004), Siberian peatlands a net carbon sink and global methane source since the early Holocene, *Science*, *303*, 353–356.
- Smith, L. C., T. M. Pavelsky, G. M. MacDonald, A. I. Shiklomanov, and R. B. Lammers (2007), Rising minimum daily flows in northern Eurasian rivers suggest a growing influence of groundwater in the high-latitude water cycle, *J. Geophys. Res.*, doi:10.1029/2006JG000327, in press.
- Striegl, R. G., M. M. Dornblaser, G. R. Aiken, K. P. Wickland, and P. A. Raymond (2007), Carbon export and cycling by the Yukon, Tanana, and Porcupine rivers, Alaska, 2001–2005, *Water Resour. Res.*, *43*, W02411, doi:10.1029/2006WR005201.
- Vedernikov, V. I., A. B. Demidov, and A. I. Sud'bin (1995), Primary production and chlorophyll in the Kara Sea in September (in English), *Oceanology*, *34*, 630–640.
- Vinogradov, M. E., V. I. Vedernikov, E. A. Romankevich, and A. A. Vetrov (2000), Components of the carbon cycle in the Russian Arctic: Primary production and flux of Corg from the photic layer (in English), *Oceanology*, *40*, 204–215.
- Wu, P., R. Wood, and P. Stott (2005), Human influence on increasing Arctic river discharges, *Geophys. Res. Lett.*, *32*, L02703, doi:10.1029/2004GL021570.
- Yang, D., B. Ye, and D. L. Kane (2004a), Streamflow changes over Siberian Yenisei River basin, *J. Hydrol.*, *296*, 59–80.
- Yang, D., B. Ye, and A. Shiklomanov (2004b), Discharge characteristics and changes over the Ob River watershed in Siberia, *J. Hydrometeorol.*, *5*, 595–610.
- Ye, H., D. Yang, T. Zhang, X. Zhang, S. Ladochy, and M. Ellison (2004), The impact of climatic conditions on seasonal river discharges in Siberia, *J. Hydrometeorol.*, *5*, 286–295.

K. Frey, Graduate School of Geography, Clark University, Worcester, MA 01610, USA. (kfrey@clarku.edu)

R. M. Holmes, Woods Hole Research Center, Falmouth, MA 02540, USA.

J. W. McClelland, Marine Science Institute, University of Texas at Austin, Port Aransas, TX 78373, USA.

L. C. Smith, Department of Geography, University of California, Los Angeles, CA 90095, USA.